Cancer Research

Neutrophil Extracellular Traps Accumulate in Peripheral Blood Vessels and Compromise Organ Function in Tumor-Bearing Animals

Jessica Cedervall[1], Yanyu Zhang[1], Hua Huang[2], Lei Zhang[2], Julia Femel[1], Anna Dimberg[2], and Anna-Karin Olsson[1]

Abstract

Cancer produces a variety of collateral effects in patients beyond the malignancy itself, including threats to distal organ functions. However, the basis for such effects, associated with either primary or metastatic tumors, are generally poorly understood. In this study, we show how heart and kidney vascular function is impaired by neutrophils that accumulate in those tissues as a result of tumor formation in two different transgenic mouse models of cancer (RIP1-Tag2 model of insulinoma and MMTV-PyMT model of breast cancer). Neutrophil depletion by systemic administration of an anti-Gr1 antibody improved vascular perfusion and prevented vascular leakage in kidney vessels. We also observed the accumulation of platelet–neutrophil complexes, a signature of neutrophil extracellular traps (NET), in the kidneys of tumor-bearing mice that were completely absent from healthy nontumor-bearing littermates. NET accumulation in the vasculature was associated with upregulation of the proinflammatory adhesion molecules ICAM-1, VCAM-1, and E-selectin, as well as the proinflammatory cytokines IL1β, IL6, and the chemokine CXCL1. Administering DNase I to dissolve NETs, which have a high DNA content, restored perfusion in the kidney and heart to levels seen in nontumor-bearing mice, and also prevented vessel leakage in the blood vasculature of these organs. Taken together, our findings strongly suggest that NETs mediate the negative collateral effects of tumors on distal organs, acting to impair vascular function, and to heighten inflammation at these sites. *Cancer Res; 75(13); 2653–62. ©2015 AACR.*

Introduction

Cancer evolves from a local disease where one or a few cells have circumvented the normal checkpoint controls and gained potential to expand in an uncontrolled manner, to a disease with systemic effects such as thrombosis, metastasis, and organ failure in the affected individual. The underlying mechanisms behind these systemic, and often fatal, consequences following growth of a primary tumor are still under intense investigation. It is clear that tumors "hijack" normal cellular functions and physiologic processes that provide a growth or survival advantage. Both the coagulation and innate immune systems can contribute to malignant development and the examples are numerous. Tissue factor (TF) is normally expressed in subendothelial spaces, and therefore only exposed to circulating blood cells after injury to the blood vessel wall. However, both tumor cells and the tumor endothelium can start to express TF, leading to thrombin generation, and hence platelet activation and coagulation in the tumor microenvironment (1). Recruitment and activation of platelets in the tumor microenvironment can promote tumor angiogenesis, growth, and dissemination by several distinct mechanisms (2, 3). Tumor-promoting properties of the M2 subtype of macrophages have been documented. In contrast with the M1, or tumor-killing macrophage, the M2 macrophages represent a major component of the tumor stroma and can promote tumorigenesis via their immunosuppressive and angiogenesis stimulating capacity (4). Similar to macrophages, subpopulations of neutrophils with either tumor-promoting or tumor-inhibitory properties have been identified (5).

Another interesting observation in this context, connecting the coagulation and innate immune systems, is the fact that neutrophil extracellular traps (NET) have been found to play a role in malignant progression (6, 7). NETs were identified in 2004 (8) and are extracellular networks that primarily consist of DNA released from neutrophils together with antimicrobial peptides and proteases derived from neutrophil granules. These NETs trap and kill bacteria and were identified as a novel mechanism by which the innate immune system efficiently protects us from infections (8). Formation of NETs, or NETosis, is critically dependent on interaction between platelets and neutrophils (9, 10). In addition to their role in microbial defense, it has during the past years become clear that NETs also form in other situations than bacterial infection, for instance, during inflammatory disease (11, 12). It was recently shown that NETs promote thrombus formation, thereby providing a link between inflammation and thrombosis (13). NETs have also been implicated in cancer-associated thrombosis and it has been shown that G-CSF secreted from the primary tumor can predispose neutrophils to NETosis (14). NET-like structures have also been found inside tumors (15) and hypothesized to play a tumor-promoting role. In a recent

[1]Department of Medical Biochemistry and Microbiology, Science for Life Laboratory, Uppsala University, Biomedical Center, Uppsala, Sweden. [2]Department of Immunology, Genetics and Pathology, Uppsala University, Rudbeck Laboratory, Uppsala, Sweden.

Note: Supplementary data for this article are available at Cancer Research Online (http://cancerres.aacrjournals.org/).

Corresponding Author: Anna-Karin Olsson, Uppsala University, Biomedical Center, Box 582, BMC, Husargatan 3, Uppsala 75123, Sweden. Phone: 46-18-471-4399; Fax: 46-18-471-4673; E-mail: anna-karin.olsson@imbim.uu.se

doi: 10.1158/0008-5472.CAN-14-3299

study by Cools-Lartigue and colleagues (16), it was described that NETs can sequester circulating tumor cells and promote metastasis (16), highlighting infection-induced NETosis as a risk factor for dissemination of a preexisting tumor.

Studies of tumor-induced effects on distant organs have primarily focused on tissues that represent metastatic sites. Interestingly, tumor-driven formation of both pro- and antimetastatic niches has been reported, which commonly involve recruitment of various types of leukocytes or bone marrow–derived cells to the metastatic site (17–20). For example, VEGFR1-positive bone marrow–derived hematopoietic progenitor cells were reported to prepare a premetastatic niche before the arrival of metastasizing tumor cells (18, 21), thus exhibiting a prometastatic function. Neutrophils were also recently shown to accumulate in the lungs before the arrival of metastatic cells in a mouse model of breast cancer. In contrast with the progenitor cells reported to promote metastasis, these so called tumor-entrained neutrophils instead counteract metastatic seeding by generating H_2O_2 and CCL2 (20). Surprisingly little is, however, known about the situation in organs that are not targets for metastasis or affected by the primary tumor. A large proportion of cancer-related deaths are, however, caused by thrombosis and general organ failure (22–24). As an example, up to 50% of multiple myeloma patients have renal failure at diagnosis (25), and acute renal failure (ARF) constitutes a major source of morbidity and mortality in cancer patients (26). For this reason, we set out to analyze tumor-induced systemic effects on distant organs, which are not directly affected by growing tumor cells. For obvious reasons human biopsy material from such tissues are rare and mouse models, therefore, become important tools for such investigations. Using two different orthotopic and spontaneously metastasizing tumor models, we analyzed the presence of blood-derived cells in organs distant from the primary tumor that do not represent metastatic sites. We found a significant increase in the number of neutrophils in heart and kidneys of tumor-bearing mice compared with healthy individuals. Moreover, vascular function was significantly impaired in these organs, a situation that was normalized upon neutrophil depletion. Platelet–neutrophil complexes, indicative of NETs, were found in kidneys from individuals with cancer. DNase treatment, which dissolves NETs due to their content of extracellular DNA, or anti–G-CSF treatment, completely restored kidney vascular function to levels seen in healthy mice. Collectively, our data strongly suggest that the impaired peripheral vessel function in individuals with cancer is due to NETosis and may contribute to cancer-induced organ failure.

Materials and Methods

Mice

Animal work was approved by the local ethics committee (C315/10, C127/13, and C77/13) and performed according to the United Kingdom Coordinating Committee on Cancer Research guidelines for the welfare of animals in experimental neoplasia. RIP1-Tag2 (genetic background C57Bl6) and MMTV-PyMT mice (genetic background FVB/n) were used for the study: Littermates lacking the transgenes, that is, healthy C57Bl6 and FVB/n mice, were used as controls. RIP1-Tag2–positive mice received drinking water supplied with 5% sucrose from ten weeks of age, to relieve hypoglycemia. For euthanization, mice were either anesthetized by i.p. injection of 2% avertin and perfused with 10 mL of 1× PBS (pH 7.4) and 10 mL of 2% paraformaldehyde (for analysis by immunostaining), or sacrificed by cervical dislocation (for RNA expression analysis). RIP1-Tag2/C57BL6 mice were analyzed at 14 weeks of age, and MMTV-PyMT mice were analyzed at 13 weeks of age. For evaluation of tumor burden, RIP1-Tag2 tumor volume was calculated using the formula $[(\pi/6) \times \text{width}^2 \times \text{length}]$. Mammary tumors from MMTV-PyMT mice were weighed immediately after dissection.

Neutrophil depletion

Neutrophil depletion was performed by i.p. injection of an anti-Ly6G antibody (Bio-X-Cell, clone RB6-8C5). Treatment was initiated in 12-week-old MMTV-PyMT mice and 13-week-old RIP1-Tag2 mice, with totally four injections of 100 μg antibody/mouse given every second day. The mice were sacrificed, as described above, one day after the last injection.

DNase treatment

DNase1 (10 U in 100 μL 0.9% NaCl; Fermentas, EN0521) was administered by i.p. injection once daily during 3 consecutive days. Treatment was initiated in 12.5 weeks old MMTV-PyMT mice and 13.5 weeks old RIP1-Tag2 mice. The mice were sacrificed, as described above, 4 to 5 hours after the last injection. Tumors and kidneys were dissected and prepared for analysis as described above.

Anti–G-CSF treatment

G-CSF was inhibited *in vivo* by i.p. injection of anti–G-CSF antibody (R&D Systems; MAB414). Treatment was initiated in 12-week-old MMTV-PyMT mice and 13-week-old RIP1-Tag2 mice. The mice were injected daily with 10 μg antibody/mouse, with a total of seven injections, and sacrificed the day after the last injection.

FITC-lectin perfusion

Perfusion of the peripheral vasculature was analyzed by lectin injection (27, 28). Briefly, FITC-conjugated lectin (Vector Laboratories; Lycopersicon Esculentum, FL-1171) was administered by retroorbital injection of 150 μL solution (0.5 mg/mL) into anesthetized mice. The solution was allowed to circulate for 2 to 3 minutes before the mice were sacrificed as described above. Tissue cryosections (kidney and heart) from mice injected with FITC-conjugated lectin were immunostained for CD31 to quantify the total vessel area. The degree of perfusion was determined by the ratio FITC-lectin–positive area/CD31-positive area, analyzed with ImageJ, revealing the proportion of vessels with functional blood flow.

Immunostainings

Cryosections fixed in ice-cold methanol were used for all immunostainings. Sections (5 μm thick) were used for all immunostainings except for those analyzed using confocal microscopy (60–80-μm thick sections). Unspecific antibody binding was blocked by 1 hour incubation with 3% BSA in 1× PBS. Primary antibody incubation was performed in room temperature for 2 hours or at 4°C overnight, followed by 45 minutes incubation with secondary antibody. Double staining for CD41 and Gr1, with both primary antibodies derived from the same species, was performed by initial staining for CD41 according to standard procedure, followed by overnight incubation at 4°C with the APC-conjugated Gr1 antibody to prevent overlapping immunoreactivity. Tissue sections were thereafter counter stained with Hoechst

(Molecular Probes, H3570) and mounted with Fluoromount-G (Southern Biotech, 0100-01).

Antibodies

The following antibodies and dilutions were used in the study: anti-CD31 (BD Biosciences; 557355, 1:1,000), anti-CD41 (BD Biosciences; 553847, 1:300), anti-fibrinogen (DakoCytomation A0080; 1:200), anti-Gr1 (BD Biosciences; 553123, 1:30), APC-conjugated anti-CD41 (BD Biosciences; 561083, 1:100), anti-CD68 (Serotec; MCA1957, 1:300), anti–ICAM-1 (R&D Systems; AF796, 1:250), and anti–VCAM-1 (R&D Systems; AF643, 1:250). Secondary antibodies: anti-goat Alexa 555 (Molecular Probes; A21431, 1:1000), anti-rabbit Alexa 586 (Molecular probes; A11011, 1:1,000), anti-rat Alexa 586 (Molecular Probes; A11077, 1:1,000), anti-rat Alexa 647 (Jackson Immuno Research; 712-605-150, 1:1,000).

Image analysis

Imaging was done on a Nikon Eclipse 90i microscope using the NIS Elements 3.2 software. Images were analyzed using the ImageJ 1.44 software (NIH). Confocal imaging was done on a Zeiss LSM 710 microscope, using the ZEN 2012 software.

Quantification of neutrophils with extracellular DNA tails

Blood cells were isolated from whole blood by centrifugation at $150 \times g$ for 15 minutes. Cells were thereafter plated on slides using cytospin (centrifugation 500 rpm, 6 minutes), fixed in ice-cold methanol and immunostained according to the protocol described above. Proportion of neutrophils undergoing NETosis was determined by staining for DNA (Hoechst) and neutrophils (Gr1), and quantification of neutrophils with secreted DNA tails related to total neutrophil count.

Quantification of DNA in plasma

DNA in plasma was quantified using the Quant-iT Picogreen dsDNA Assay Kit (Life Technologies, P7589), according to the manufacturer's instructions. Blood samples were collected by heart puncture, and plasma was isolated by centrifugation at $1{,}100 \times g$ for 10 minutes.

RNA extraction and qRT-PCR

The expression of proinflammatory mediators and endothelial activation markers was analyzed by qPCR on RNA extracted from kidneys. qPCR was also used to determine expression of G-CSF in primary tumors from MMTV-PyMT mice, RIP1-Tag2 mice, and C57BL6 mice with subcutaneously grafted B16 melanoma. RNA was extracted from kidney and tumor tissue using the RNeasy Midi Kit (Qiagen; 75142). Tissues were homogenized in lysis buffer and RNA was isolated and purified according to the procedure recommended by the manufacturer. RT-PCR was performed using the SuperScript III Reverse Transcriptase (Invitrogen, 18080-044). SYBR Green (Life Technologies, 4309155) was used for the qPCR reaction. The genes and associated primers used for qPCR are listed in Supplementary Table S1.

Statistical analysis

Statistical analysis was performed using Prism (GraphPad Software Inc.). The nonparametric two-tailed Mann–Whitney analysis was used to compare data in various groups. Correlation analysis was performed using the Spearman correlation test; *, $P \leq 0.05$; **, $P \leq 0.01$; ***, $P \leq 0.001$.

Results

Mice with tumors display impaired vascular function in peripheral tissue

Systemic vascular effects of cancer were analyzed using two well-established transgenic mouse models; the MMTV-PyMT mouse model developing mammary carcinomas with subsequent metastatic spread primarily to the lung, and the RIP1-Tag2 mouse developing carcinomas in the insulin-producing cells of the pancreas, with metastatic spread to lung and liver. Analysis of renal tissue from these tumor-bearing mice demonstrated a significantly impaired vascular perfusion, measured by injection of FITC-conjugated lectin, compared with healthy control mice without tumors (MMTV-PyMT: $P = 0.0358$; RIP1-Tag2: $P = 0.0002$; Fig. 1A). Vascular function was further analyzed by immunostaining for extravasated fibrinogen, allowing evaluation of the degree of leakage from the renal vasculature. Both MMTV-PyMT and RIP1-Tag2 mice displayed increased vascular leakage compared with healthy mice lacking tumors (MMTV-PyMT: $P = 0.0417$; RIP1-Tag2: $P = 0.0004$; Fig. 1B). These results clearly demonstrate that tumor-bearing individuals display a remarkably impaired function of the vasculature in a peripheral tissue not directly affected by the primary tumor or metastases.

Peripheral vascular perfusion correlates with primary tumor size

As described above, perfusion of the renal vasculature was found to be significantly impaired in two different mouse models of cancer. However, although the MMTV-PyMT mice all displayed a low perfusion, RIP1-Tag2 mice clearly formed two separate groups; one group of mice with extremely poor perfusion (5%–30%), and one group with perfusion corresponding well with the control mice lacking tumors (around 80%; Fig. 1A, bottom right). Interestingly, a correlation between perfusion of the renal vasculature and size of the primary tumors was found. Mice with primary tumor volumes larger than 100 mm^3 had significantly impaired perfusion compared with mice with tumor volumes below 100 mm^3 ($P = 0.0355$; Fig. 1C). This suggests that primary tumor burden is an important factor for the systemic vascular effects seen in tumor-bearing mice.

Increased neutrophil infiltration in kidneys from tumor-bearing mice

To determine whether the reduced peripheral vessel function in mice with cancer was mediated via altered infiltration of immune cells, kidney sections from MMTV-PyMT mice were immunostained for detection of macrophages (CD68), neutrophils (Gr1), and platelets (CD41). Neutrophil infiltration was significantly increased in renal tissue from tumor-bearing mice compared with tumor-free control mice (MMTV-PyMT: $P = 0.0159$; RIP1-Tag2: $P = 0.0085$; Fig. 2A). Platelet numbers in the kidneys were not significantly altered, although there was a trend toward increased platelet numbers in kidneys from MMTV-PyMT mice (Fig. 2B). A similar result was observed for infiltrating macrophages, where MMTV-PyMT mice demonstrated a slight but not significant increase (MMTV-PyMT: $P = 0.1714$; RIP1-Tag2; $P = 0.9714$; Fig. 2C). Interestingly, a significant correlation was found between primary tumor weight and the number of neutrophils infiltrating the kidney glomeruli of MMTV-PyMT mice, suggesting that the

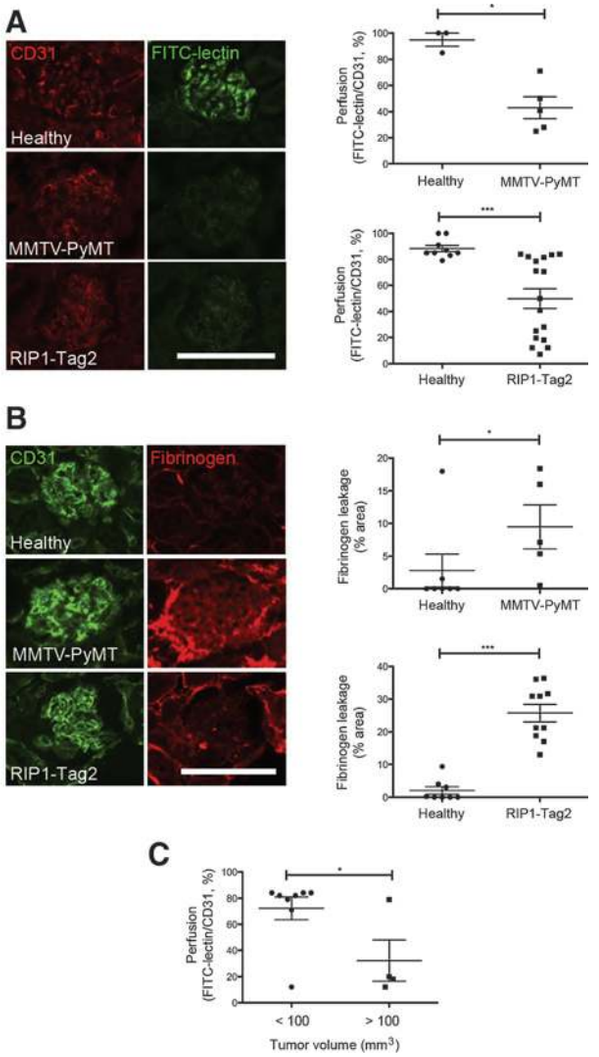

Figure 1.
Decreased perfusion and increased leakage from the renal vasculature in mice with cancer. Kidney vascular perfusion and leakage was analyzed in the transgenic mouse tumor models MMTV-PyMT and RIP1-Tag2. A, perfusion, assessed by injection of FITC-lectin, was significantly decreased in kidneys from both models compared with healthy control mice. B, immunostaining for extravasated fibrinogen revealed significantly increased vascular leakage from vessels in tumor-bearing mice. RIP1-Tag2 mice displayed a correlation between primary tumor size and vascular perfusion in the kidneys; mice with tumor volumes below 100 mm^3 had renal perfusion comparable with healthy control mice, whereas mice with tumor volume above 100 mm^3 demonstrated significantly impaired perfusion (C). Each data point corresponds to one individual mouse. Original magnification, ×20; scale bars, 100 μm; *, $P \leq 0.05$; ***, $P \leq 0.005$.

primary tumor may promote neutrophil infiltration in a distant organ ($P = 0.0108$; Fig. 2D).

Neutrophil depletion improves function of the renal vasculature in tumor-bearing mice

The results described above show that the decrease in renal vascular function is paralleled with increased neutrophil infiltration in mice with cancer. To investigate whether the increased neutrophil infiltration was linked to the impaired vascular function, MMTV-PyMT and RIP1-Tag2 mice were neutrophil depleted by injection of an antibody against the neutrophil cell surface marker Gr1. Successful neutrophil depletion was verified by immunostaining (Supplementary Fig. S1A). Neutrophil depletion significantly improved function of the renal vasculature, as illustrated by increased FITC-lectin perfusion (MMTV-PyMT: $P = 0.0399$; RIP1-Tag2: $P = 0.0465$; Fig. 3A and Supplementary Fig. S2A) and reduced vascular leakage (MMTV-PyMT: $P = 0.0295$; RIP1-Tag2: $P = 0.0052$; Fig. 3B and Supplementary Fig. S2B). Altogether, this indicates that neutrophils are important as mediators of the tumor-induced effects on peripheral vessel function.

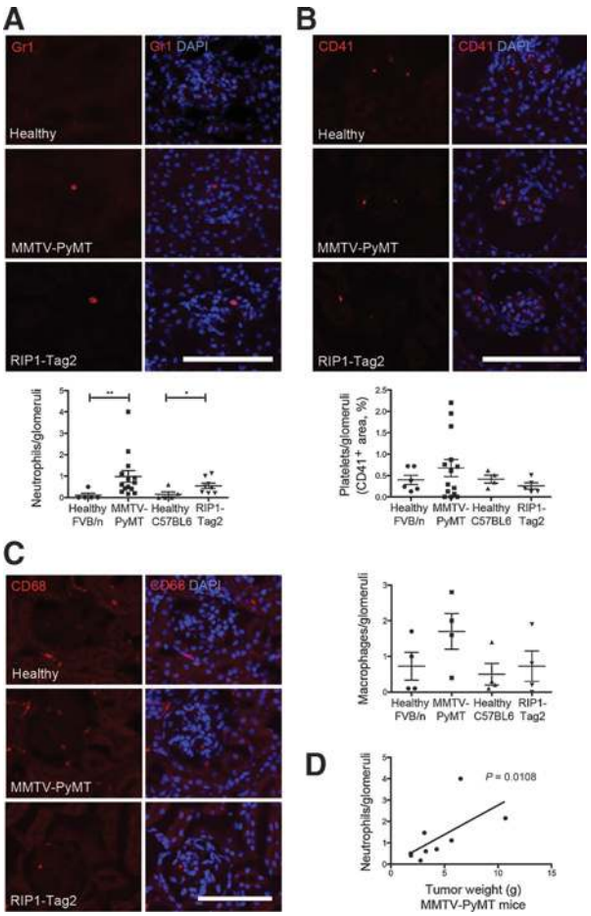

Figure 2.
Enhanced neutrophil infiltration in kidney glomeruli in mice with tumors. Immunostaining for neutrophils (A; Gr1), platelets (B; CD41), and macrophages (C; CD68) in kidneys from MMTV-PyMT and RIP1-Tag2 mice revealed a significantly increased number of neutrophils in kidney glomeruli from both MMTV-PyMT and RIP1-Tag2 mice (A). B, MMTV-PyMT mice did also show a trend toward increased numbers of platelets compared with healthy control mice of the same genetic background, whereas those numbers were unaltered in RIP1-Tag2 mice. C, macrophage numbers were not significantly altered in any of the transgenic tumor models, although a slight increase was observed in MMTV-PyMT mice. D, the number of neutrophils in kidney glomeruli from MMTV-PyMT mice significantly correlated with size of the primary tumors. Each data point corresponds to one individual mouse. Original magnification, ×20; scale bars, 100 μm; *, $P \leq 0.05$; **, $P \leq 0.01$.

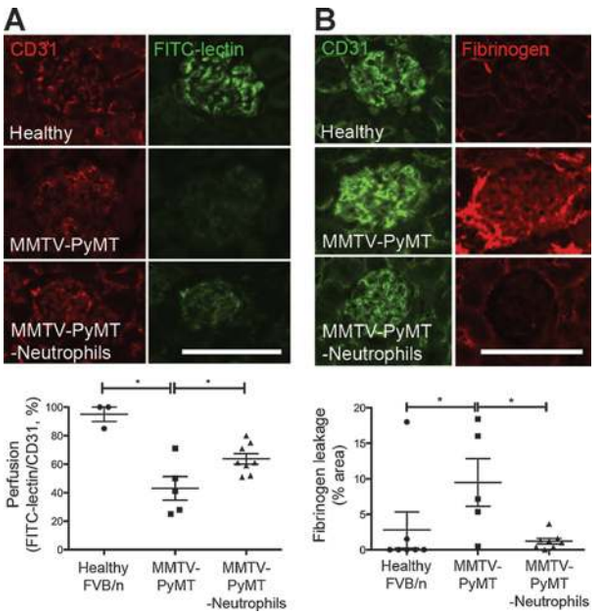

Figure 3.

Neutrophil depletion improves perfusion and prevents leakage from the renal vasculature of tumor-bearing mice. Neutrophil depletion of MMTV-PyMT mice using an antibody against Gr1 resulted in significantly improved renal perfusion (A) and decreased vascular leakage to levels comparable with healthy control mice (B). Each data point corresponds to one individual mouse. Original magnification, ×20; scale bars, 100 μm; *, $P \leq 0.05$.

NETs are responsible for the tumor-induced negative effects on peripheral vascular function

As previously described, platelet numbers were not significantly increased in kidneys from tumor-bearing mice. However, doublestaining for neutrophils and platelets demonstrate neutrophil–platelet complex formation in renal tissue sections from both RIP1-Tag2 and MMTV-PyMT mice (Fig. 4A). This phenomenon could not be observed in any of the analyzed healthy control mice. Neutrophils and platelets are known to colocalize in NETs; web-like structures composed by neutrophil-secreted extracellular DNA and neutrophil-derived proteases (10). NET formation was originally described as a microbial defense mechanism, but recently cancer was also described as a NET-inducing factor (14). To investigate whether the neutrophil–platelet aggregates detected in renal tissue from tumor-bearing mice could be NETs, MMTV-PyMT mice were treated with DNase, a well-established method to dissolve NETs, for 3 days. The DNase treatment resulted in a significant reduction of the number neutrophil–platelet complexes in the kidneys of MMTV-PyMT mice ($P = 0.0049$; Fig. 4A), suggesting that these complexes are indeed NETs. Analysis of kidney sections with confocal microscopy revealed that the NETs were almost exclusively localized within the renal vasculature (Fig. 4B). The intravascular location of the neutrophil–platelet complexes were also asessed in optical sections from three different angles, further supporting this finding (Fig. 4C). To further support that NETs are present in the circulation of tumor-bearing mice, neutrophils from peripheral blood were stained for Gr1 and DNA, and the proportion of neutrophils with extracellular DNA tails was determined. The results revealed a significantly higher number of neutrophils with DNA tails in tumor-bearing mice compared with healthy mice ($P = 0.0294$; Fig. 4D). In line with this, elevated levels of circulating DNA was found in plasma from tumor-bearing mice ($P = 0.0489$; Fig. 4E). Perfusion and vascular leakage in kidneys from DNase treated tumor-bearing mice was further analyzed to elucidate whether NETs may be responsible for the negative effects on peripheral vessel function. Indeed, perfusion of the renal vasculature was restored in these mice to levels comparable with tumor-free mice (MMTV-PyMT: $P = 0.0159$; RIP1-Tag2: $P = 0.0026$; Fig. 5A and Supplementary Fig. S3A). In parallel, the increased fibrinogen leakage in tumor-bearing mice was completely abolished after DNase treatment (MMTV-PyMT, $P = 0.0079$; RIP1-Tag2, $P = 0.0022$; Fig. 5B and Supplementary Fig. S3B). DNase treatment did not suppress the total number of neutrophils in the kidney (Fig. 5C), but decreased the proportion of neutrophils aggregating with platelets (Fig. 4A). These results demonstrate that neutrophils impair vascular function in the kidneys of tumor-bearing mice by forming NETs. The intravascular localization of the complexes indicates that NETs prevent efficient perfusion by vessel occlusion.

To explore whether our observations were specific for kidney or also applied to other organs in an individual with cancer, we analyzed FITC-lectin perfusion of heart, because this tissue is not a metastatic site in the MMTV-PyMT model. Again, we found a significantly reduced vascular perfusion in tumor-bearing mice compared with healthy littermates (Fig. 6A) and an elevated number of neutrophils in the heart (Fig. 6B). Neutrophil depletion or DNase treatment resulted in normalized perfusion, indistinguishable from healthy individuals (Fig. 6A). Neutrophil numbers were not affected by the DNase treatment (Fig. 6B). These data strongly suggest that cancer-induced systemic and intravascular NET formation reduces vascular function in organs not directly affected by the primary tumor or metastases.

A potentially important tumor-derived factor in this context is G-CSF, which was recently reported to predispose neutrophils for NET formation (14). C57BL6 mice with subcutaneously grafted B16 melanoma tumors did not display decreased perfusion or increased leakage of the renal vasculature and only a slight, but nonsignificant increase in neutrophil infiltration compared with healthy control mice (Supplementary Fig. S4A–S4C). Quantification of neutrophil–platelet complexes revealed that some complexes were formed in mice with B16 tumors, but the proportion of neutrophils aggregating with CD41 was significantly lower compared with the proportion in MMTV-PyMT mice ($P = 0.0061$; Supplementary Fig. S4D). Interestingly, qPCR for G-CSF revealed a strong expression of G-CSF in MMTV-PyMT tumors, whereas expression in B16 tumors was negligible in comparison (Supplementary Fig. S4E). RIP1-Tag2 tumors expressed approximately 10 times more G-CSF than B16 melanoma. These results support the hypothesis that the increased NET formation is driven by G-CSF produced by the primary tumor. To test this hypothesis directly, we treated MMTV-PyMT mice with an anti–G-CSF antibody daily during a week before analyzing renal vascular perfusion and neutrophil–platelet complex formation. Anti–G-CSF treatment restored vascular perfusion of the kidney vasculature and reduced complex formation between platelets and neutrophils (Supplementary Fig. S5A and S5B), further supporting a role for G-CSF in tumor-induced impairment of peripheral vessel function.

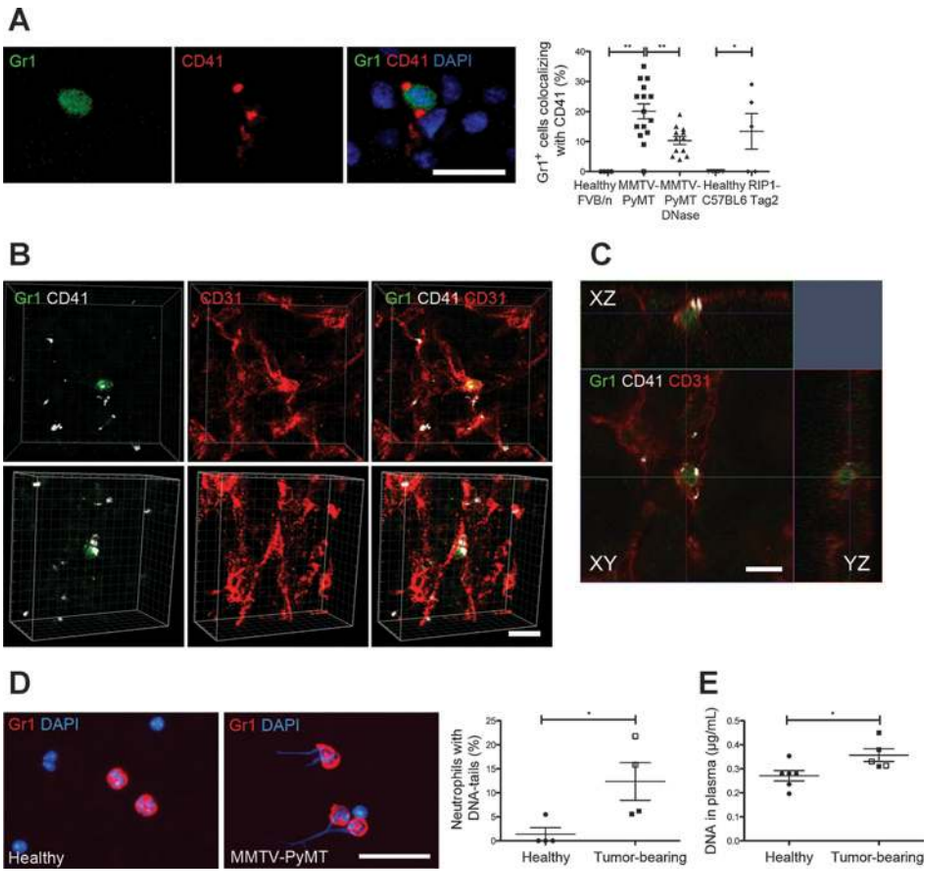

Figure 4.
Neutrophils from tumor-bearing mice form NETs localizing within the kidney vasculature. A, immunostaining for neutrophils (Gr1) and platelets (CD41) revealed neutrophil–platelet aggregates in kidneys from tumor-bearing mice, a phenomenon not observed in any healthy control mice. DNase treatment, which dissolves NETs, significantly reduced the proportion of neutrophils in complex with platelets in kidneys from MMTV-PyMT mice. B, confocal microscopy showed that a majority of the complexes were located inside the vessels, as illustrated here by two different examples. C, the intravascular presence of colocalizing neutrophils/platelets was further verified in optical sections allowing analysis from three different angles (XY, XZ, and YZ). D, cytospin preparations of neutrophils from mice with and without tumors stained for Gr1 and DNA (Hoechst), and the proportion of neutrophils with extracellular DNA tails was significantly higher in tumor-bearing mice than healthy littermates. E, the concentration of circulating DNA was also increased in mice with tumors. D and E, filled squares represent MMTV-PyMT mice and empty squares represent RIP1-Tag2 mice. Each data point corresponds to one individual mouse. Original magnification, ×20; scale bar in A, 20 μm and in all other figures 10 μm; *, $P \leq 0.05$; **, $P \leq 0.01$.

Increased endothelial activation and expression of proinflammatory cytokines in kidneys from mice with cancer

Our results demonstrate that mice with tumors have strikingly poor vascular perfusion of the kidneys. Maintenance of a continuous blood flow is essential for regulating endothelial activity. This suggests that kidneys from mice with tumors could have an altered activation status of their vascular endothelium, which in turn may promote inflammation. To determine whether endothelial activation is increased in renal vasculature from MMTV-PyMT mice, RNA expression levels for the endothelial adhesion molecules ICAM-1, VCAM-1 and E-selectin were analyzed in kidneys by qPCR. The results show significantly increased RNA expression for ICAM-1 ($P = 0.0159$), VCAM-1 ($P = 0.0317$) and E-selectin ($P = 0.0079$; Fig. 7A). To further assess the inflammatory status in kidneys from tumor-bearing mice, qPCR analysis of a panel of 15 cytokines and chemokines (Supplementary Table S1) involved in neutrophil recruitment and inflammatory responses, was performed. We found a significant upregulation of the proinflammatory cytokines IL1β ($P = 0.0079$; Fig. 7B), IL6 ($P = 0.0079$; Fig. 7C), and CXCL1 ($P = 0.0317$; Fig. 7D) in kidneys from MMTV-PyMT mice, as compared with kidneys from healthy mice. Upregulation of these soluble factors and adhesion molecules likely provides an explanation for the increased presence of neutrophils in the kidneys of RIP1-Tag2 and MMTV-PyMT mice. DNase treatment suppressed the expression of E-selectin, IL1β, IL6, and CXCL1 to levels comparable with those of healthy littermates (Fig. 7A–D). In line with this, some of the DNase-treated mice showed a marked reduction in expression of ICAM-1 and VCAM-1, and the significant upregulation detected in tumor-bearing mice was lost (Fig. 7A). Together these molecular data clearly show that an inflammatory response can be induced in a "healthy" organ in an individual with cancer, as a result of tumor-induced systemic effects.

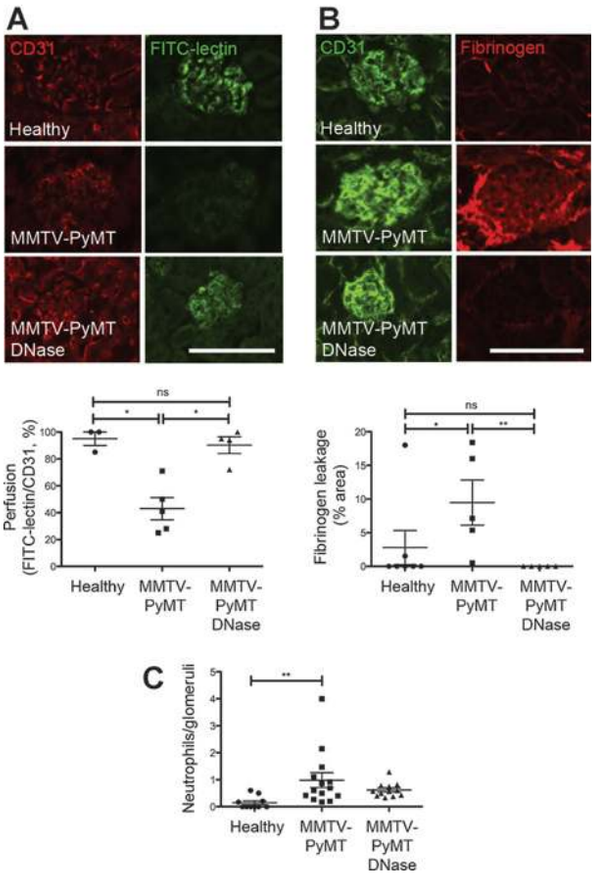

Figure 5.
NETs mediate decreased vascular function in tumor-bearing mice. Vascular function was completely restored after DNase treatment as judged by normalized FITC-lectin perfusion (A) and suppressed fibrinogen extravasation (B) of MMTV-PyMT mice. Increased neutrophil infiltration was not suppressed by DNase treatment (C). Each data point corresponds to one individual mouse. Original magnification, ×20; scale bar in A, 20 μm and in all other figures 100 μm; *, $P \leq 0.05$; **, $P \leq 0.01$; ns, nonsignificant.

Discussion

Cancer mortality is mainly connected to systemic effects induced by the primary tumor such as metastasis, deep vein thrombosis, and a general organ failure. Because of these tumor-induced effects on the systemic environment in an individual with cancer, we aimed to investigate potential changes with respect to vascular function and inflammation in organs that are not targets for metastasis or affected by the primary tumor. Using the two orthotopic and metastasizing models RIP1-Tag2 for insulinoma and MMTV-PyMT for breast cancer, both believed to closely resemble disease development in the human situation, we found a dramatic reduction in the vascular function in kidney and heart compared with healthy littermates of the same genetic background (FVB/n and C57BL6). In some individuals, renal perfusion was as low as 5% to 30%, but with an average 50% reduction compared with mice without tumors. Moreover, there was a 5- to 10-fold increase in the amount of extravasated fibrinogen in the kidney, indicative of vascular leakage. We found these data unexpected, but looking into the situation in humans it is, however, clear that there is a high incidence of renal complications as a consequence of cancer or its treatment (29, 30). ARF is a cause of substantial morbidity in cancer patients and is indeed characterized by hypoperfusion of the kidney vasculature (25).

In addition to the reduced vascular functionality, we found a significantly elevated number of $Gr1^+$ neutrophils in heart and kidney tissue from mice with cancer. These neutrophils were strongly associated to the observed vascular effects, because depletion of $Gr1^+$ cells normalized kidney vascular function in both RIP1-Tag2 and MMTV-PyMT mice. Even more striking was the effect of DNase treatment, which completely restored perfusion and prevented leakage in kidney and heart vasculature, resulting in a perfusion indistinguishable from the healthy individual. DNase treatment did not significantly alter the total number of neutrophils in the kidney or heart of tumor-bearing mice but reduced the number of neutrophil–platelet complexes, suggesting that NETs are the cause of the impaired vascular function in individuals with cancer. G-CSF has been reported to predispose neutrophils to form NETs (31) and tumor-derived G-CSF has been implicated as a possible cause of cancer-related thrombosis by priming circulating neutrophils to undergo NETosis (14). In agreement, we found no impairment of peripheral vessel function or increased neutrophil infiltration in kidneys

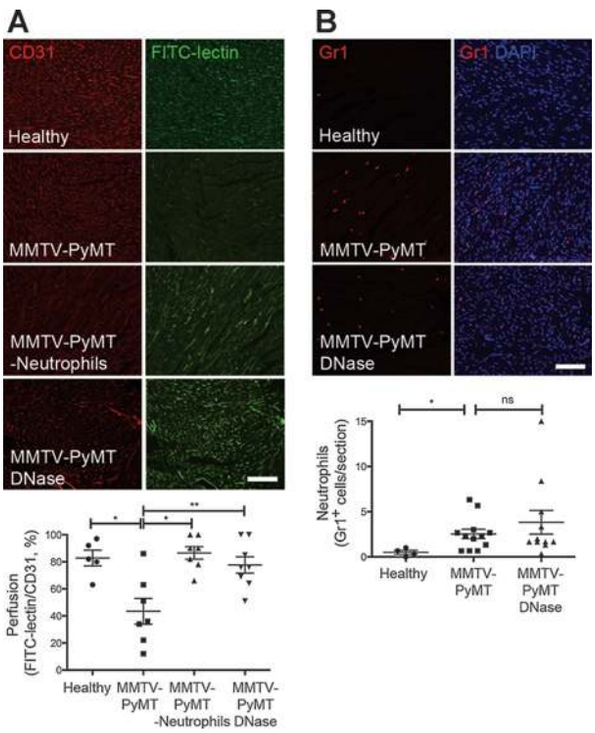

Figure 6.
Impaired vascular function and increased neutrophil infiltration in heart tissue from MMTV-PyMT mice. FITC-lectin perfusion of heart tissue was significantly impaired in MMTV-PyMT mice compared with healthy control mice; an effect that could be reversed by neutrophil depletion or DNase treatment (A). In accordance with results from kidney analysis, the number of infiltrating neutrophils in the heart was significantly increased in MMTV-PyMT mice compared with healthy littermates and was not changed upon DNase treatment (B). Each data point corresponds to one individual mouse. Original magnification, ×20; scale bars, 100 μm; *, $P \leq 0.05$; **, $P \leq 0.01$; ns, nonsignificant.

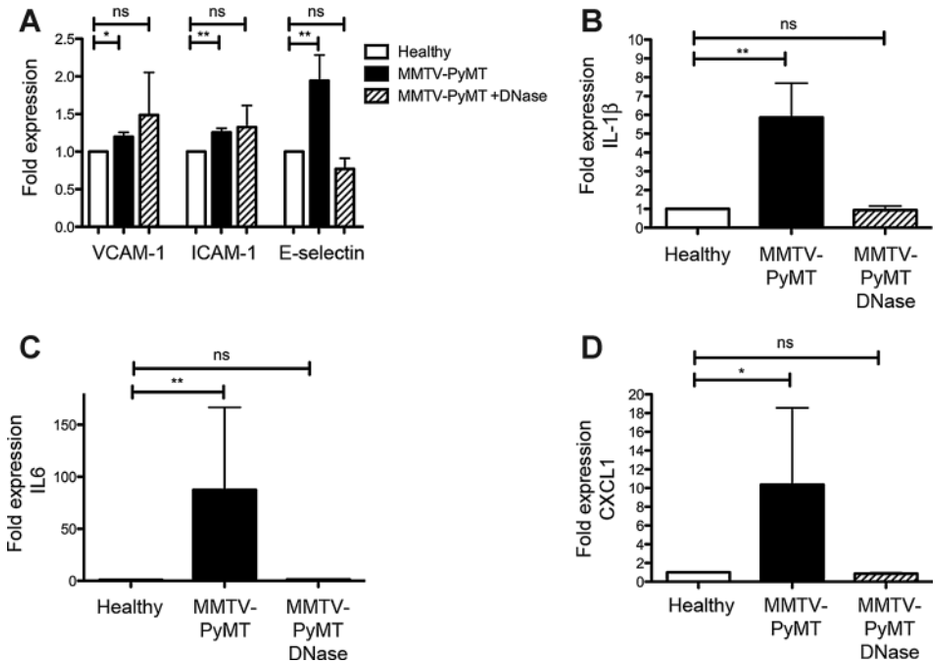

Figure 7.
Endothelial adhesion molecules and inflammatory cytokines are upregulated in kidneys from MMTV-PyMT mice. A, expression analysis by qPCR of the endothelial activation markers VCAM, ICAM, and E-selectin revealed significant upregulation of these adhesion molecules in kidneys from MMTV-PyMT mice. The inflammatory status of kidneys from MMTV-PyMT mice was analyzed by qPCR for a panel of different cytokines (Supplementary Table S1) and showed increased expression of several proinflammatory mediators; IL1β expression was increased six times (B), IL6 expression was increased 87 times (C), and CXCL1 expression was increased 10 times (D), compared with RNA levels in kidneys from healthy littermates. DNase treatment completely suppressed the increased expression of E-selectin (A), IL1β (B), IL6 (C), and CXCL1 (D) in the kidneys from all mice, whereas some but not all mice showed a suppressed expression of ICAM-1 and VCAM-1. *, $P \leq 0.05$; **, $P \leq 0.01$; ns, nonsignificant.

from mice with subcutaneous B16 melanoma, a tumor type that expressed very low levels of G-CSF compared with MMTV-PyMT tumors (220-fold difference) and RIP1-Tag2 tumors (10-fold difference). Moreover, administration of an anti–G-CSF antibody during one week restored kidney vascular perfusion of MMTV-PyMT mice. These data further support NETosis as a cause of the impaired vascular function in distant organs in mice with cancer.

By which mechanisms could NETs cause impaired function of the vasculature? NETs are reported to be cytotoxic for endothelium and to directly induce endothelial cell damage (9, 32). These harmful effects on endothelium by NETs are likely caused by the release of proteases such as elastase and myeloperoxidase. Impaired perfusion could also create an ischemic condition in small vessels, thereby causing endothelial cell damage. In addition, histones, which are present in the NETs, have been demonstrated to exert endothelial cell cytotoxicity (33). We could however not detect any increased apoptosis in kidney endothelium from mice with tumors compared with healthy littermates (data not shown), but this does not exclude an elevated endothelial cell death due to other mechanisms than apoptosis. It is, however, possible that the decreased blood perfusion we detected in distant organs in mice with cancer is simply a consequence of small occlusions in the microvessels, generated by NETs. The latter suggestion is supported by the fact that DNase treatment restored vascular function and reverted the inflammatory phenotype in kidneys of tumor-bearing mice.

A change in blood flow can affect the activation state of the endothelium and induce an upregulated expression of adhesion molecules, promoting influx of inflammatory cells. Indeed, we could detect elevated expression levels of ICAM-1, VCAM-1, and E-selectin in the kidneys of mice with tumors. Moreover, we found increased transcriptional levels of the inflammatory cytokines IL1β and IL6, as well as the chemokine CXCL1. These molecules are important mediators of inflammatory responses and are expressed by leukocytes and platelets, but also epithelial cells and tumor cells in the case of CXCL1 (34–36). CXCL1 possesses strong neutrophil chemoattractant capacity (36). Both IL1β and IL6 are also expressed by tubular epithelial cells in diseased kidneys (37, 38). In line with this, IL1β and IL6 are overexpressed in kidneys from mice with ARF induced by ischemia or cisplatin treatment (39–41). The importance of IL6 in ARF has been demonstrated in IL6-deficient mice (39). Mice lacking IL6 display reduced endothelial ICAM-1 expression and neutrophil infiltration in renal tissues, paralleled with less histologic signs of tubular injury, upon experimentally induced ARF (39). Increased expression of CXCL1, IL1β, and IL6 in the kidney of tumor-bearing mice indicates an ongoing inflammatory response, with a molecular signature resembling ARF. Interestingly, DNase treatment reverted this inflammatory phenotype in the kidneys from tumor-bearing mice, indicating that NETs are causing these changes. The fact that the proinflammatory state was reversible, is encouraging from a therapeutic perspective and suggests that DNase could potentially be a useful drug to prevent tumor-induced systemic inflammation and possibly organ failure. DNase is already in clinical use for the management of cystic

fibrosis, where DNA containing debris is collected in the lungs, demonstrating its safety as a drug (42).

On the basis of our data, we believe that the sequence of events leading to reduced perfusion of peripheral vessels in individuals with cancer are initiated by tumor secreted factors (likely G-CSF but additional soluble molecules may also play a role), which promote NET formation in the periphery, causing a reduced blood perfusion in distant organs and as a consequence upregulation of leukocyte adhesion markers in the vasculature. This would further add to the inflammatory state by recruiting leukocytes to the affected tissue. It is, therefore, possible that we look at two different populations of neutrophils in kidney and heart tissue from tumor-bearing mice; (i) neutrophils engaged in intravascular NETosis and (ii) neutrophils that have extravasated and infiltrated the kidney tissue as a result of upregulation of vascular adhesion molecules.

Tumor vessels have been demonstrated to exhibit a reduced expression of endothelial adhesion molecules, mainly caused by an increased exposure to proangiogenic molecules such as VEGF and bFGF in the tumor microenvironment (43). Dirkx and colleagues (44) also report on tumor-induced systemic suppression of leukocyte–vessel wall interaction, although less pronounced compared with the situation within the tumor. This systemic effect was also assumed to be caused by circulating proangiogenic factors, but not directly addressed. Although the finding in Dirkx and colleagues may seem in contrast with our finding of a tumor-induced upregulation of endothelial adhesion markers, there are several possible explanations for this discrepancy. First of all, tumor-induced NETosis and subsequent impairment of peripheral vessel function does not occur in all tumor types, as exemplified in our study by the subcutaneous B16 melanoma model. Mice with B16 tumors display very limited platelet–neutrophil complexes in the kidney and no impairment of the renal vascular perfusion. Moreover, B16 tumors do not express G-CSF, a molecule that promotes NET formation. Clearly, there is a dependency on tumor type for systemic NETosis and the subsequent peripheral vascular effects we find. In the study by Dirkx and colleagues, B16 melanoma was used in addition to the human colon carcinoma cell line LS174T in immunocompromised mice. We have no information on G-CSF expression in LS174T, and it is uncertain if human G-CSF would be equally potent as mouse G-CSF in eliciting host NETosis. Second, the study by Dirkx and colleagues analyzed total leukocyte–vessel wall interaction within the ear vasculature, whereas we measure expression of adhesion molecules, as well as neutrophil infiltration, in the kidney. To address a potentially upregulated VEGFR2 signaling in kidneys of tumor-bearing mice, derived from tumor-secreted VEGF in the circulation, we performed imunostainings with an antibody recognizing the complex of VEGFA and VEGFR2 (GV39M), but did not find an elevated signal compared with kidneys from healthy mice (data not shown). A recent publication also nicely demonstrate that due to polarization of VEGFR1/2 expression—VEGFR1 on the luminal side and VEGFR2 on the abluminal side of blood vessels (45), VEGF in the circulation is less likely to affect the endothelium compared with VEGF coming from the tumor tissue (abluminal side).

In conclusion, our data strongly suggest that the impaired peripheral vessel function we detect in individuals with cancer is due to formation of intravascular NETs. It is possible that tumor-induced NETosis is a contributing factor to general organ failure commonly seen in cancer patients. This process may be more or less pronounced depending on tumor type–specific expression of soluble factors promoting NET formation. It is clear that tumor-induced impacts on distant organs are not limited to metastatic sites. One could speculate that the tumor-induced effects on peripheral vasculature we observe does play a role in metastasis, but that the actual growth and survival of the metastatic cells in an organ is critically dependent on the correct microenvironment. Considering that cancer mortality is mainly due to systemic effects induced by the primary tumor, including dissemination to distant organs, thrombotic events, and organ failure, increased knowledge of these processes are warranted to improve current therapeutic strategies.

Disclosure of Potential Conflicts of Interest

No potential conflicts of interest were disclosed.

Authors' Contributions

Conception and design: J. Cedervall, A. Dimberg, A.-K. Olsson
Development of methodology: J. Cedervall, Y. Zhang, H. Huang, A.-K. Olsson
Acquisition of data (provided animals, acquired and managed patients, provided facilities, etc.): J. Cedervall, Y. Zhang, H. Huang, L. Zhang, J. Femel, A.-K. Olsson
Analysis and interpretation of data (e.g., statistical analysis, biostatistics, computational analysis): J. Cedervall, Y. Zhang, A.-K. Olsson
Writing, review, and/or revision of the manuscript: J. Cedervall, J. Femel, A. Dimberg, A.-K. Olsson
Administrative, technical, or material support (i.e., reporting or organizing data, constructing databases): J. Cedervall, Y. Zhang
Study supervision: A. Dimberg, A.-K. Olsson

Acknowledgments

The authors thank the kind supply of tumor tissue from Dr. Elise Langenkamp, Uppsala University, and Prof. Kristian Pietras, Lund University, Sweden.

Grant Support

This study was supported by The Swedish Cancer Society #11 0653 and the Swedish Research Council #2010-6903-75363-44 (A.-K. Olsson) and #2012-77PK-22157-01-2 (J. Cedervall).

The costs of publication of this article were defrayed in part by the payment of page charges. This article must therefore be hereby marked *advertisement* in accordance with 18 U.S.C. Section 1734 solely to indicate this fact.

Received November 10, 2014; revised March 2, 2015; accepted March 30, 2015; published OnlineFirst June 12, 2015.

References

1. Lip GY, Chin BS, Blann AD. Cancer and the prothrombotic state. Lancet Oncol 2002;3:27–34.
2. Cedervall J, Olsson A-K. Platelet regulation of angiogenesis, tumor growth and metastasis, ed. S. Ran. Tumor Angiogenesis 2012:115–34. InTech, DOI: 10.5772/29318. Available from: http://www.intechopen.com/books/tumor-angiogenesis/platelet-regulation-of-angiogenesis-tumor-growth-and-metastasis.
3. Sharma D, Brummel-Ziedins KE, Bouchard BA, Holmes CE. Platelets in tumor progression: a host factor that offers multiple potential targets in the treatment of cancer. J Cell Physiol 2014;229:1005–15.

4. Sica A, Schioppa T, Mantovani A, Allavena P. Tumour-associated macrophages are a distinct M2 polarised population promoting tumour progression: potential targets of anti-cancer therapy. Eur J Cancer 2006; 42:717–27.
5. Gregory AD, Houghton AM. Tumor-associated neutrophils: new targets for cancer therapy. Cancer Res 2011;71:2411–6.
6. Demers M, Wagner DD. NETosis: a new factor in tumor progression and cancer-associated thrombosis. Semin Thromb Hemost 2014;40:277–83.
7. Cools-Lartigue J, Spicer J, Najmeh S, Ferri L. Neutrophil extracellular traps in cancer progression. Cell Mol Life Sci 2014;71:4179–94.
8. Brinkmann V, Reichard U, Goosmann C, Fauler B, Uhlemann Y, Weiss DS, et al. Neutrophil extracellular traps kill bacteria. Science 2004;303:1532–5.
9. Clark SR, Ma AC, Tavener SA, McDonald B, Goodarzi Z, Kelly MM, et al. Platelet TLR4 activates neutrophil extracellular traps to ensnare bacteria in septic blood. Nat Med 2007;13:463–9.
10. Phillipson M, Kubes P. The neutrophil in vascular inflammation. Nat Med 2011;17:1381–90.
11. Gupta AK, Hasler P, Holzgreve W, Gebhardt S, Hahn S. Induction of neutrophil extracellular DNA lattices by placental microparticles and IL-8 and their presence in preeclampsia. Hum Immunol 2005;66: 1146–54.
12. Kessenbrock K, Krumbholz M, Schonermarck U, Back W, Gross WL, Werb Z, et al. Netting neutrophils in autoimmune small-vessel vasculitis. Nat Med 2009;15:623–5.
13. Fuchs TA, Brill A, Duerschmied D, Schatzberg D, Monestier M, Myers DD Jr, et al. Extracellular DNA traps promote thrombosis. Proc Natl Acad Sci U S A 2010;107:15880–5.
14. Demers M, Krause DS, Schatzberg D, Martinod K, Voorhees JR, Fuchs TA, et al. Cancers predispose neutrophils to release extracellular DNA traps that contribute to cancer-associated thrombosis. Proc Natl Acad Sci U S A 2012;109:13076–81.
15. Ho-Tin-Noe B, Carbo C, Demers M, Cifuni SM, Goerge T, Wagner DD. Innate immune cells induce hemorrhage in tumors during thrombocytopenia. Am J Pathol 2009;175:1699–708.
16. Cools-Lartigue J, Spicer J, McDonald B, Gowing S, Chow S, Giannias B, et al. Neutrophil extracellular traps sequester circulating tumor cells and promote metastasis. J Clin Invest. 2013 Jul 1. [Epub ahead of print].
17. Hiratsuka S, Nakamura K, Iwai S, Murakami M, Itoh T, Kijima H, et al. MMP9 induction by vascular endothelial growth factor receptor-1 is involved in lung-specific metastasis. Cancer Cell 2002;2:289–300.
18. Kaplan RN, Riba RD, Zacharoulis S, Bramley AH, Vincent L, Costa C, et al. VEGFR1-positive haematopoietic bone marrow progenitors initiate the pre-metastatic niche. Nature 2005;438:820–7.
19. Kang SY, Halvorsen OJ, Gravdal K, Bhattacharya N, Lee JM, Liu NW, et al. Prosaposin inhibits tumor metastasis via paracrine and endocrine stimulation of stromal p53 and Tsp-1. Proc Natl Acad Sci U S A 2009; 106:12115–20.
20. Granot Z, Henke E, Comen EA, King TA, Norton L, Benezra R. Tumor entrained neutrophils inhibit seeding in the premetastatic lung. Cancer Cell 2011;20:300–14.
21. Kaplan RN, Psaila B, Lyden D. Bone marrow cells in the `pre-metastatic niche': within bone and beyond. Cancer Metastasis Rev 2006;25:521–9.
22. Prandoni P, Falanga A, Piccioli A. Cancer and venous thromboembolism. Lancet Oncol 2005;6:401–10.
23. McFadden ME, Sartorius SE. Multiple systems organ failure in the patient with cancer. Part I: pathophysiologic perspectives. Oncol Nurs Forum 1992;19:719–24.
24. Cho H, Mariotto AB, Mann BS, Klabunde CN, Feuer EJ. Assessing non-cancer-related health status of US cancer patients: other-cause survival and comorbidity prevalence. Am J Epidemiol 2013;178:339–49.
25. Darmon M, Ciroldi M, Thiery G, Schlemmer B, Azoulay E. Clinical review: specific aspects of acute renal failure in cancer patients. Crit Care 2006; 10:211.
26. Lameire NH, Flombaum CD, Moreau D, Ronco C. Acute renal failure in cancer patients. Ann Med 2005;37:13–25.
27. Huang J, Frischer JS, Serur A, Kadenhe A, Yokoi A, McCrudden KW, et al. Regression of established tumors and metastases by potent vascular endothelial growth factor blockade. Proc Natl Acad Sci U S A 2003;100: 7785–90.
28. Inai T, Mancuso M, Hashizume H, Baffert F, Haskell A, Baluk P, et al. Inhibition of vascular endothelial growth factor (VEGF) signaling in cancer causes loss of endothelial fenestrations, regression of tumor vessels, and appearance of basement membrane ghosts. Am J Pathol 2004;165:35–52.
29. Humphreys BD, Soiffer RJ, Magee CC. Renal failure associated with cancer and its treatment: an update. J Am Soc Nephrol 2005;16:151–61.
30. Aapro M, Launay-Vacher V. Importance of monitoring renal function in patients with cancer. Cancer Treat Rev 2012;38:235–40.
31. Yousefi S, Mihalache C, Kozlowski E, Schmid I, Simon HU. Viable neutrophils release mitochondrial DNA to form neutrophil extracellular traps. Cell Death Differ 2009;16:1438–44.
32. Villanueva E, Yalavarthi S, Berthier CC, Hodgin JB, Khandpur R, Lin AM, et al. Netting neutrophils induce endothelial damage, infiltrate tissues, and expose immunostimulatory molecules in systemic lupus erythematosus. J Immunol 2011;187:538–52.
33. Xu J, Zhang X, Pelayo R, Monestier M, Ammollo CT, Semeraro F, et al. Extracellular histones are major mediators of death in sepsis. Nat Med 2009;15:1318–21.
34. Rider P, Carmi Y, Guttman O, Braiman A, Cohen I, Voronov E, et al. IL-1alpha and IL-1beta recruit different myeloid cells and promote different stages of sterile inflammation. J Immunol 2011;187:4835–43.
35. Scheller J, Chalaris A, Schmidt-Arras D, Rose-John S. The pro- and anti-inflammatory properties of the cytokine interleukin-6. Biochim Biophys Acta 2011;1813:878–88.
36. Kobayashi Y. The role of chemokines in neutrophil biology. Front Biosci 2008;13:2400–7.
37. Fukatsu A, Matsuo S, Yuzawa Y, Miyai H, Futenma A, Kato K. Expression of interleukin 6 and major histocompatibility complex molecules in tubular epithelial cells of diseased human kidneys. Lab Invest 1993; 69:58–67.
38. Tesch GH, Yang N, Yu H, Lan HY, Foti R, Chadban SJ, et al. Intrinsic renal cells are the major source of interleukin-1 beta synthesis in normal and diseased rat kidney. Nephrol Dial Transplant 1997;12: 1109–15.
39. Patel NS, Chatterjee PK, Di Paola R, Mazzon E, Britti D, De Sarro A, et al. Endogenous interleukin-6 enhances the renal injury, dysfunction, and inflammation caused by ischemia/reperfusion. J Pharmacol Exp Ther 2005;312:1170–8.
40. Faubel S, Lewis EC, Reznikov L, Ljubanovic D, Hoke TS, Somerset H, et al. Cisplatin-induced acute renal failure is associated with an increase in the cytokines interleukin (IL)-1beta, IL-18, IL-6, and neutrophil infiltration in the kidney. J Pharmacol Exp Ther 2007;322:8–15.
41. Liu M, Chien CC, Burne-Taney M, Molls RR, Racusen LC, Colvin RB, et al. A pathophysiologic role for T lymphocytes in murine acute cisplatin nephrotoxicity. J Am Soc Nephrol 2006;17:765–74.
42. Thomson AH. Human recombinant DNase in cystic fibrosis. J R Soc Med 1995;88 Suppl 25:24–9.
43. Griffioen AW, Damen CA, Blijham GH, Groenewegen G. Tumor angiogenesis is accompanied by a decreased inflammatory response of tumor-associated endothelium. Blood 1996;88:667–73.
44. Dirkx AE, Oude Egbrink MG, Kuijpers MJ, van der Niet ST, Heijnen VV, Bouma-ter Steege JC, et al. Tumor angiogenesis modulates leukocyte-vessel wall interactions *in vivo* by reducing endothelial adhesion molecule expression. Cancer Res 2003;63:2322–9.
45. Hudson N, Powner MB, Sarker MH, Burgoyne T, Campbell M, Ockrim ZK, et al. Differential apicobasal VEGF signaling at vascular blood-neural barriers. Dev Cell 2014;30:541–52.